World Applied Sciences Journal 9 (10): 1191-1200, 2010
ISSN 1818-4952

Large-Eddy Simulations of Three Dimensional Turbulent Jet in a Cross Flow Using A Dynamic Subgrid-Scale Eddy Viscosity Model with a Global Model Coefficient

[1]*M. Taeibi-Rahni*, [2]*M. Ramezanizadeh*, [1]*A. Darvan*, [3]*D.D. Ganji*,
[3]*Soheil Soleimani*, [3]*E. Ghasemi and* [3]*H. Bararnia*

[1]Islamic Azad University, Science and Research Branch of Tehran, Tehran, Iran
[2]Department of Aerospace Engineering, Air University of Shahid Sattari, Iran
[3]Department of Mechanical Engineering, Babol University of Technology, Babol, Iran

Abstract: An eddy-viscosity subgrid-scale model proposed by Vreman [1] applied in large-eddy simulation of a jet in a cross-flow problem to investigate the turbulent flow structure and the vortex dynamics. The model is essentially not more complicated than the Smagorinsky model, but is constructed in such a way that its dissipation is relatively small in transitional and near-wall regions. The model is expressed in first-order derivatives, does not involve explicit filtering, averaging, or clipping procedures and is rotationally invariant for isotropic filter widths. Because of these highly desirable properties the model seems to be well suited for engineering applications. Unlike the Smagorinsky model, the present model is able to adequately handle not only turbulent but also transitional flow. A turbulent flat plate boundary layer at a Reynolds number of Re=4700 interacts with a jet issued from a pipe. Finite volume method (FVM) using SIMPLE algorithm is implemented in this simulation. The numerical outcomes are compared with experimental results and Reynolds Averaged Navier-Stokes (RANS) approach. The LES results are in much better agreement with the existing experimental ones, in comparison with computational results of the RANS.

Key words: Large-eddy simulation · Dynamic subgrid-scale eddy-viscosity · Jet-in-a-crossflow

INTRODUCTION

Jet into cross flow simulation has relevance to active flow control, which is presently an area of intense interest in the research community. It has several applications, including pollutants dilution, flame stabilization, fluid mixing, the take-off or landing behavior of V/STOL airplanes and gas turbine blade surface protection from hot gas flow, namely film cooling, etc. There are several parameters affecting the characteristics of jets into a cross flow, such as injection angle, relative spacing of the injection holes, velocity ratio, density ratio, state of the oncoming boundary layer, ratio of the boundary layer thickness to the injection hole diameter, surface curvature, longitudinal pressure gradient and free stream turbulence level, etc. Among these, the penetration of jets into the main flow depends strongly on the jets to cross flow velocity ratio, R and/or injection angle, α. For large α's and R's, the flow is of a wake character and is similar to the flow past a solid cylinder placed on the wall. Downstream of the bending-over jet, a reverse flow zone develops, in which the hot gas is mixed in from the sides. Past the reversed-flow zone, the jet reattaches on the surface. On the other hand, at small velocity ratios, the jet bends over very quickly and attaches to the wall. Also, when the injection angle is small, the jet attaches quickly to the wall, while at higher velocity ratios, the flow develops a characterizing wall-jet. Jet penetration and the mixing characteristics of multiple jets into a cross flow are three-dimensional phenomena and have been the object of research for many years [2-15]. Andreopoulos [2] presented spectral analysis and flow visualization for various velocity ratios and Reynolds numbers of a jet issuing perpendicularly from a developing pipe flow into a cross flow. His experimental investigations revealed the existence of large-scale structures in the jet flow. These structures were sometimes well organized, depending, basically, on the Reynolds number and the jet to cross flow velocity ratio. He also noted that, at high velocity ratios, say R>3 and low Reynolds numbers, say Re < 5000,

Corresponding Author: A. Darvan, Islamic Azad University, Science and Research Branch of Tehran, P.O. Box 14155-4933.
Tel/Fax: +98 111 3234205, E-mail: ali_darvan.amiri@yahoo.com.

the annular mixing layer of the pipe rolls and toroidal vortices are formed, similar to those of a jet issuing into `still' air. These well organized vortices, or vortical rings (large structures), carry a vorticity of the same sign as the ones inside the pipe, but opposite to those of the cross-stream turbulent flow. As the velocity ratio decreases, the organization of these large structures reduces, but still there exists a periodicity in their appearance. As the Reynolds number increases, say $Re > 5000$, the regularity of the appearance of the large structures leaving the pipe decreases and the eddies now have a wide range of sizes. Finally, the average vorticity content of jets into a cross flow far downstream of the jet exit seems to be qualitatively independent of the Reynolds number for velocity ratios less than about 2.0. Lee *et al.* [3] conducted an experimental study to investigate the flow characteristics of streamwise 35° inclined jets, injected into a turbulent cross flow boundary layer of a at plate. In their work, the flow was visualized by Schlieren photographs, for both normal and inclined jets, to determine the overall flow structure with the variation of the velocity ratio. They measured the three-dimensional velocity field for two velocity ratios of 1.0 and 2.0, using a five-hole directional probe. Their visualization study showed that the variation of the injection angle causes a significant change in the flow structure. Also, they found that the jet flow is mainly dominated by turbulence for small velocity ratios, but is likely to be influenced by inviscid vorticity dynamics for large velocity ratios. Also, a pair of bound vortices accompanied by a complex three-dimensional flow is present downstream of the jet exit, as in the case of the normal injection whose range and strength depend on the velocity ratio. They concluded that the three-dimensional flow characteristics are so dominated that the previous two-dimensional measurements in the symmetry plane are not sufficient to account for the flow structure of the jets into the cross flow, especially for large velocity ratios. Their work also showed that, when the velocity ratio is small, the fluid from the jet exit is bent towards the wall. Therefore, it seems that only the injected fluid in some downstream region of the jet exit exists. However, for large velocity ratios, the injected jet is separated from the wall abruptly, such that only the cross flow fluid is filled in the region between the wall and the jet trajectory. Ajersch *et al.* [4] have both experimentally and computationally studied the flow of a row of six square jets injected perpendicularly to a cross flow. Their jet to cross flow velocity ratios were 0.5,1.0 and 1.5, while their jet spacing to jet width ratio was 3.0. Also, their jet Reynolds number was 4700. They measured the mean velocities and the six Reynolds stresses, using a three-component Laser Doppler Velocimeter (LDV) operating in coincidence mode. Their computational flow simulation was performed using a multi-grid, segmented, $k-\varepsilon$ computational fluid dynamic code. Their special near wall treatment included a non-isotropic formulation of the effective viscosity, a low Reynolds number model for k and an algebraic model of the flow length scale. Their computational domain included the jet channel, as well as the flow above it. In their work, the flow velocities and Reynolds stresses on the jet centerline, downstream of the jet exit, were not predicted very well, probably due to the inadequate turbulence model used. However, the values off the centerline matched reasonably well with those of their experiments. Holdeman and Walker [5] developed an empirical model for predicting the temperature distribution downstream of a row of dilution jets injected normally into a heated cross flow in a constant area duct. Their model was based on the assumption that all properly non-dimensionalized vertical temperature profiles can be expressed in a self-similar form. They claimed that their results were in excellent agreement with the experimental data, except for the combinations of the flow and the geometric variables, which resulted in a strong impingement on the opposite wall. Hoda and Acharya [6] studied the performance of seven different existing turbulence models (a high-Re model, three low-Re models, two non-linear models and a Direct Numerical Simulation (DNS) based low-Re model) for the prediction of film coolant jets injected normally into a cross flow. They compared their results of different models with the experimental data of Ajersch *et al.* [3] and with each other to critically evaluate the performance of those models. They claimed that close agreement with the experimental results were obtained at the jet exit and far downstream of the injection region using different models. However, all models used typically over-predicted the magnitude of the velocities in the wake region behind the jet. Keimasi and Taeibi-Rahni [7] also computationally studied a three-dimensional turbulent flow of jets injected perpendicularly into a cross flow. They applied the Reynolds averaged Navier-Stokes equations in general form, using the SIMPLE finite volume method over a non-uniform staggered grid, including the jet channel. Their results of two different turbulence models used (standard $k-\varepsilon$ with wall function and zonal $(k-\varepsilon)/(k-\omega)$) were compared with the previous existing computational and experimental results for three different velocity ratios of 0.5,1.0 and 1.5. They reported that the mean velocity profiles agreed well with the experimental data, whereas there were some discrepancies in the turbulence kinetic energy profiles. Acharya *et al*. [8] studied the capabilities of different predictive methods ($k-\varepsilon$) models, Reynolds Stress Transport Model (RSTM), Large Eddy Simulation (LES) and (DNS) in correctly calculating the measured statistics of a film cooling jet in a cross flow. They only simulated the cross flow and applied the experimental inlet boundary condition at the jet exit. They reported that two-equation models usually underpredict the lateral spreading of the film cooling jet and overpredict its vertical prediction. Their RSTM predictions were not substantially better than their two-equation model predictions. Finally, they reported that the LES and DNS predictions were better able to predict the mean velocities and the turbulent stresses.

Formulation of the Problem: The dimensionless Navier-Stokes equations for incompressible, three-dimensional and time-dependent flow are, as follows:

$$\partial_i u_i = 0,$$
$$\partial_t u_i + \partial_k(u_i u_k) = -\partial_i p + \frac{1}{\mathrm{Re}}\partial_{kk} u_i. \tag{1}$$

The governing LES equations are obtained by filtering the above equations. Filtration is a process by which all scales smaller than a selected size, e.g., grid size is eliminated from the total flow and, hence, the resolvable part of the flow is defined. This process is accomplished using a general filter function in space to limit the range of scales in the flow field. The one dimensional filter function procedure is:

$$\bar{f}(x) = \frac{1}{\Delta x}\int f(x_1)G(x, x_1)dx_1,$$

$$\bar{f}(x) = f(x) - f'(x) \tag{2}$$

Where:

$f'(x)$ is the subgrid scale (SGS) component of the flow variable, $f(x)$. Applying the above filter operation to the Navier-Stokes equations, the LES equations are derived as:

$$\partial_i \bar{u}_i = 0,$$

$$\partial_t \bar{u}_i + \partial_k(\bar{u}_i \bar{u}_k) = -\partial_i \bar{p} + \frac{1}{\mathrm{Re}}\partial_{kk}\bar{u}_i - \partial_j \tau_{ij}. \tag{3}$$

The effects of the small scales are present throughout the SGS stress tensor,

$$\tau_{ij} = \left(\overline{u_i u_j} - \bar{u}_i \bar{u}_j\right) \tag{4}$$

which requires to be modeled [16-20].

Subgrid Scale Model: The development of subgrid models for large-eddy simulation (LES) is an important area in turbulence research [21, 22]. Eddy-viscosity models are popular, since they are robust in practice and principally respect the dissipative character of turbulence. An accurate eddy viscosity for inhomogeneous turbulent flow should become small in laminar and transitional regions. This requirement is unfortunately not satisfied by existing simple eddy viscosity closures such as the well-known Smagorinsky model [23]. Germano *et al*. [24]solved this problem by the application of a dynamic procedure to the Smagorinsky model. The common implementation of the dynamic procedure incorporates explicit filtering operations, ensemble averaging in homogeneous directions and a somewhat *ad hoc* clipping to prevent an unstable (negative) eddy viscosity. The extension of these techniques to complex flows is not trivial, which is an important reason to continue the search for an eddy viscosity that performs reasonably well without additional procedures. LES with an eddy-viscosity closure solves the filtered Navier–Stokes equations

$$\partial_j \bar{u}_j = 0, \tag{5}$$

$$\partial_t \bar{u}_i + \partial_j(\bar{u}_i \bar{u}_j) = -\partial_i(\bar{p} + \tau_{kk}/3) + \nu \partial_j^2 \bar{u}_i + \partial_j(2\nu_e S_{ij}), \tag{6}$$

, using the summation convention for repeated indices. The unknown turbulent stress tensor

$$\tau_{ij} = \left(\overline{u_i u_j} - \bar{u}_i \bar{u}_j\right) \tag{7}$$

has been replaced by the model

$$-2\nu_e S_{ij} + \tau_{kk}\delta_{ij}/3 \tag{8}$$

Where: $S_{ij} = \frac{1}{2}\partial_i \bar{u}_j + \partial_j \bar{u}_i$

The following eddy viscosity is proposed in the present paper:

$$v_e = c\sqrt{\frac{B_\beta}{\alpha_{ij}\alpha_{ij}}}, \tag{9}$$

with

$$\alpha_{ij} = \partial_i \overline{u}_j = \frac{\partial \overline{u}_j}{\partial x_i}, \tag{10}$$

$$\beta_{ij} = \Delta^2{}_m \alpha_{mi}\alpha_{mj}, \tag{11}$$

$$\beta_{ij} = \beta_{11}\beta_{22} - \beta_{12}^2 + \beta_{11}\beta_{33} - \beta_{13}^2 + \beta_{22}\beta_{33} - \beta_{23}^2. \tag{12}$$

The model constant c is related to the Smagorinsky constant C_s by $c \approx 2.5C_s^2$. Like the Smagorinsky model, this model is easy to compute in actual LES, since it does not need more than the local filter width and the first-order derivatives of the velocity field. The symbol α represents the (3 ×) matrix of derivatives of the filtered velocity $\overline{u}$. If α_{ij} α_{ij} equals to zero, v_e is consistently defined as zero. The tensor β is proportional to the gradient model [25] in its general anisotropic form [26]. It is positive semidefinite [27, 28] which implies $B_\beta \geq 0$. In fact, B_β is an invariant of the matrix β, while α_{ij} α_{ij} is an invariant (trace) of $\alpha^T\alpha$. Therefore, model (5) is invariant under a rotation of the coordinate axes, in case the filter width is the same in each direction ($\Delta_i = \Delta$ implies $\beta = \Delta^2\alpha^T\alpha$).

Numerical Procedure: The present computational methodology includes a finite volume method, using SIMPLE algorithm, employing a multi-block and non-uniform staggered grid. It should be noted that in the interface of the two blocks of crossflow and jet flow, the grid points are located exactly in the same locations. A power law differencing scheme is used for the convective and diffusive terms and the fully implicit scheme is applied for the time discretization It should be noted that the computational domain and its boundary conditions are selected based on the experimental and computational work of Ajersch *et al.* [4], which is used as one of our benchmarks. A 1/7 power law velocity profile is considered at the cross flow inlet, where uniform flow at the jet inlet is used. Also, uniform time step of $t = 0.01$ is considered for time marching to t = 72 second. Note that we have used the time averages of the results for the present work for our investigations. The proposed computational domain and its boundary conditions and the computational grid are shown in Figures 1 and 2,

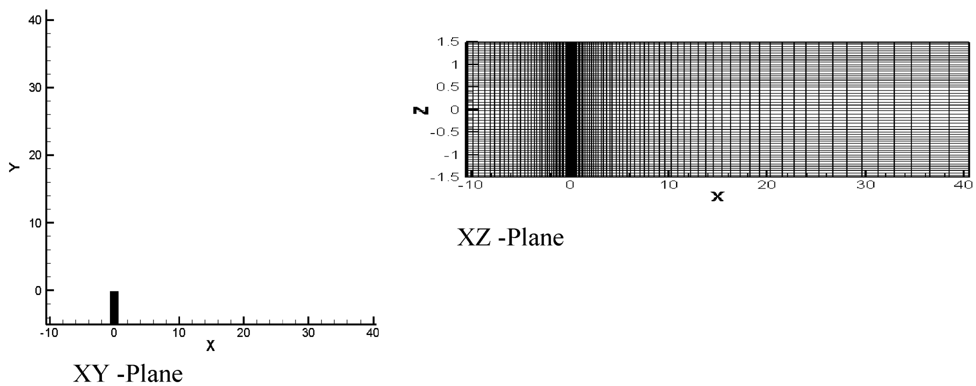

Fig. 1: Computational grid

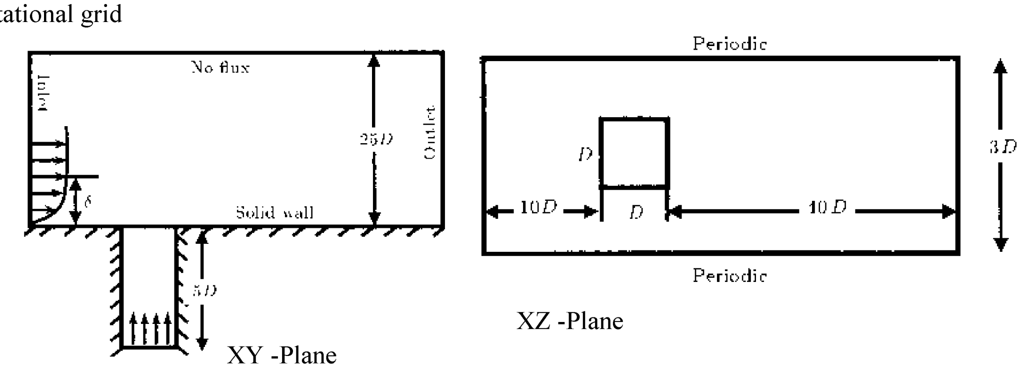

Fig. 2: Computational domain and its boundary conditions.

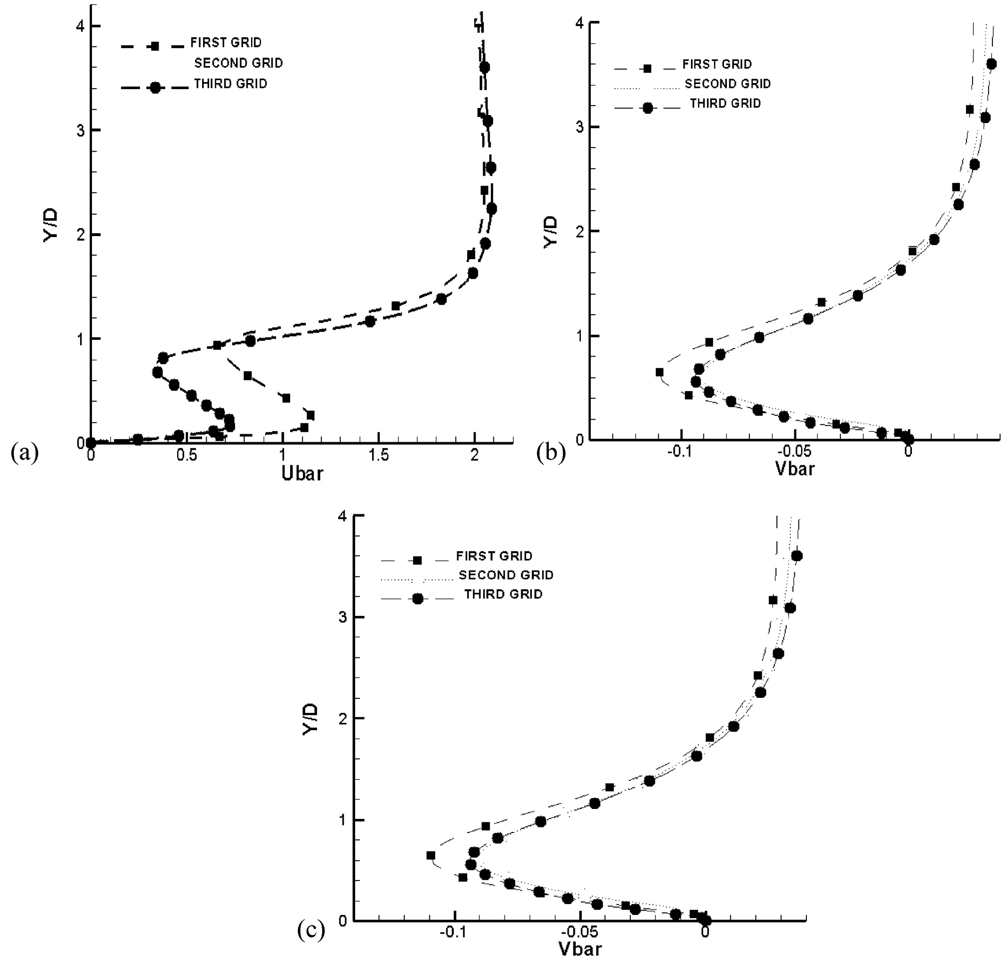

Fig. 3: Grid study of velocity profiles at different *YZ* -planes (*X/D* = (a) 0.0, (b) -1.0 and (c) -5.0) at *Z/D* = 0.0 plane

Table 1: Grid arrangements for grid resolution study

Bocks	Jet Flow Block			Cross Flow Block		
Direction	X	Y	Z	X	Y	Z
First grid	8	33	9	80	72	24
Second grid	10	34	10	90	79	35
Third grid	15	21	15	100	90	55

respectively. The Cartesian coordinate system is used in which *X* is parallel to the cross flow direction, *Y* is parallel to the initial jet flow direction and *Z* is perpendicular to the *XY*-plane. Note that the origin of the coordinate system is located on the geometrical center of the jet exit. The cross flow boundary layer thickness used is the same as that used in Ajersch's experimental work (δ = 2D). As shown in Figure 1, a single square cross-section jet is considered in the computational domain. To impose the influences of the other jets, the periodic boundary condition is used in the Z-direction. Fig. 3 depicts the three grid study for velocity profiles at different *YZ*-planes (X / D = (a) 0.0, (b) -1.0 and (c) -5.0) at Z / D = 0.0 plane and also the grid resolution study is performed using different grid arrangements Table 1.

RESULTS AND DISCUSSION

Numerical simulation of jet in a cross flow, for velocity ratio, 0.5 has been performed using LES approach. No temperature difference between the jet and the cross flow is considered. The jet Reynolds number is 4700 and, thus, the injected flow is turbulent. Note that, in almost all previous works [8], the cross flow alone has been solved using an existing boundary condition at the jet exit, while it seems to be necessary to solve the flow in the jet channel along with the cross flow, simultaneously. Fig. 3 displays the mean streamwise velocity profiles, $<\overline{U}>$, for different *X* locations at Z / D = 0.0.As it is obvious, the present numeric simulation (LES) is in excellent agreement

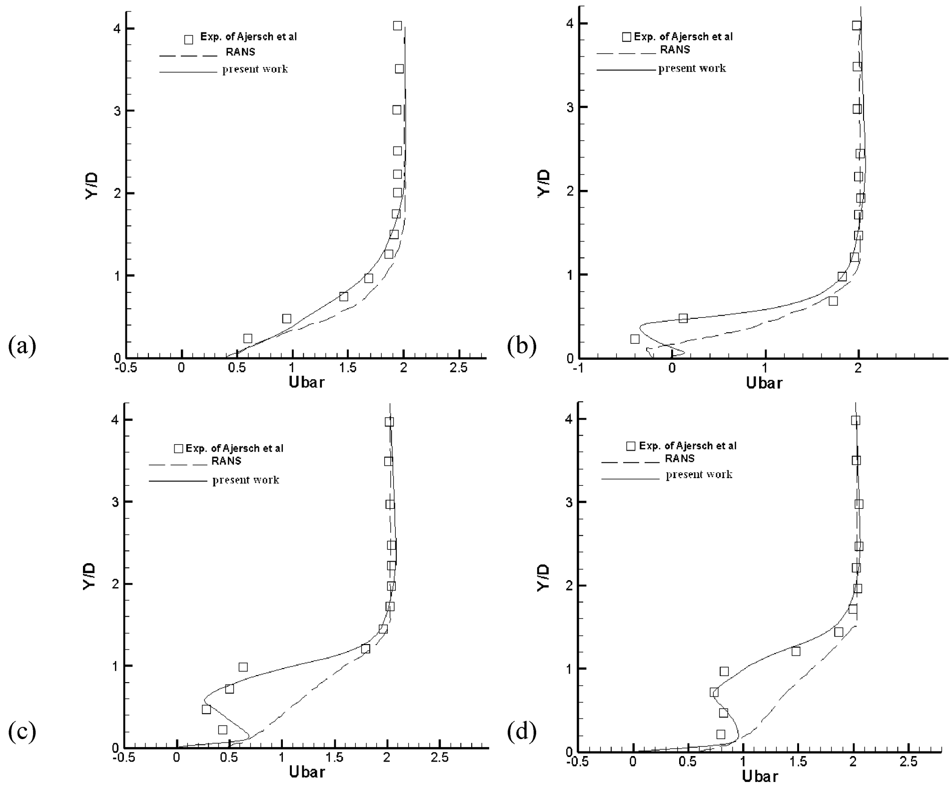

Fig. 4: $<\overline{U}>$ -velocity profiles of R = 0.5 at different *YZ*-planes (*X/D* = (a) 0.0, (b) 1.0, (c) 3.0 and (d) 5.0) at *Z/D*= 0.0 plane

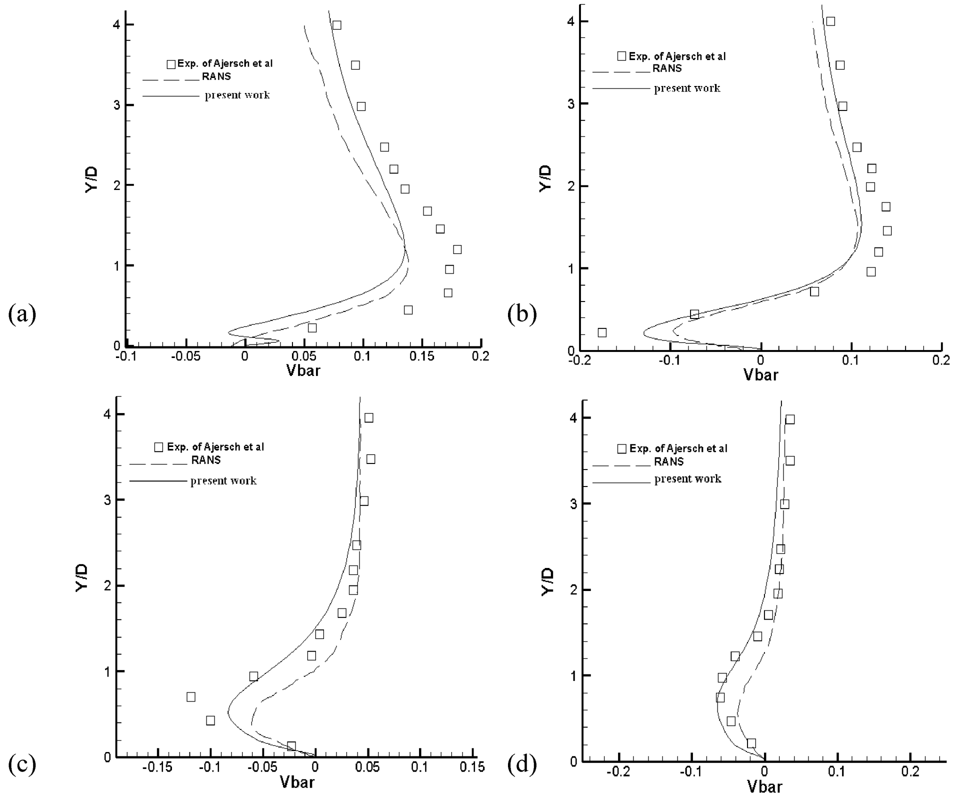

Fig. 5: $<\overline{V}>$ -velocity profiles of R = 0.5 at different *YZ*-planes (*X/D*= (a) 0.0, (b) 1.0, (c) 3.0 and (d) 5.0) at *Z/D*= -1.0 plane

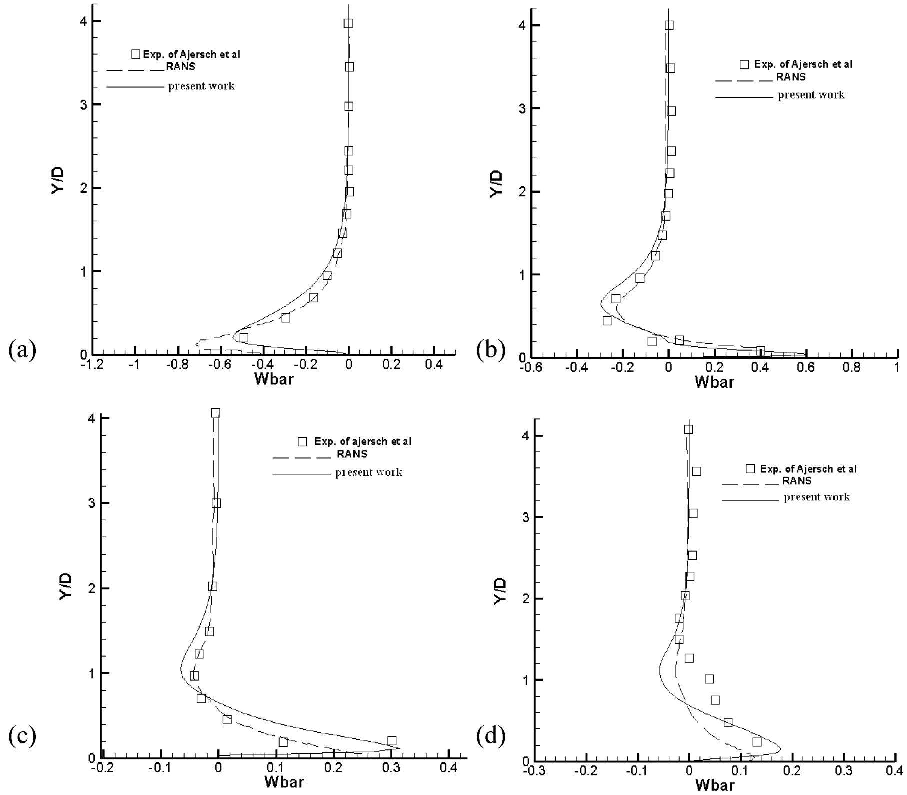

Fig. 6: $<\overline{W}>$-velocity profiles of R = 0.5 at different *YZ*-planes (*X/D* = (a) 0.0, (b) 1.0, (c) 3.0 and (d) 5.0) at *Z/D*= -0.5 plane

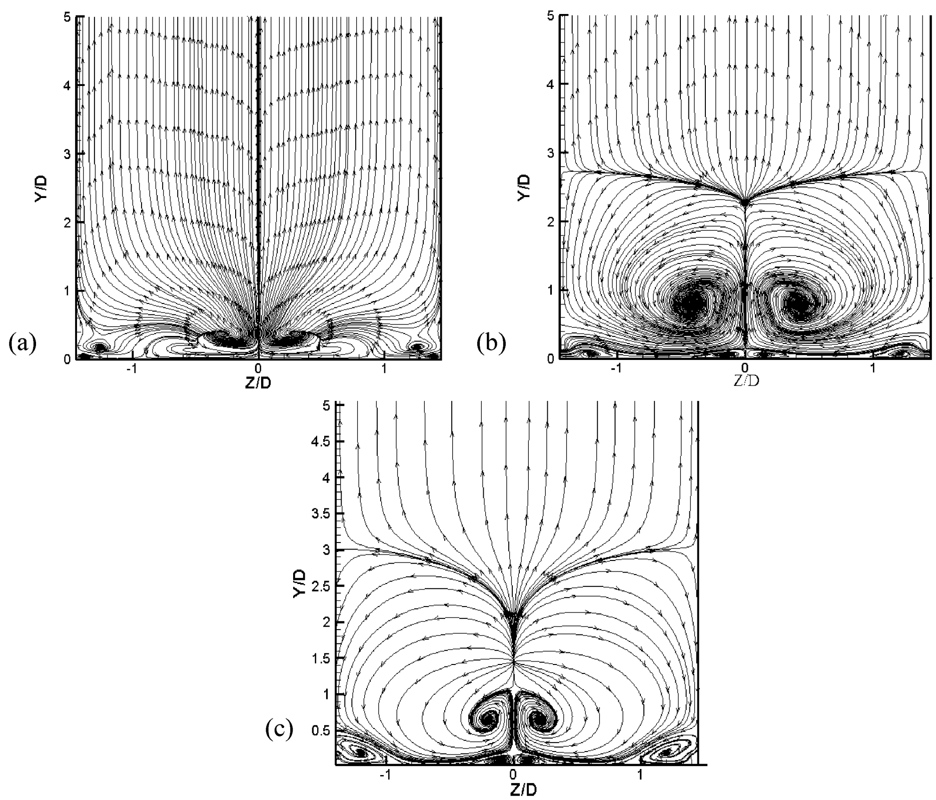

Fig. 7: The flow streamlines for different *YZ*-planes (*X/D* = (a) 1.0, (b) 5.0) and (c) 8.0.

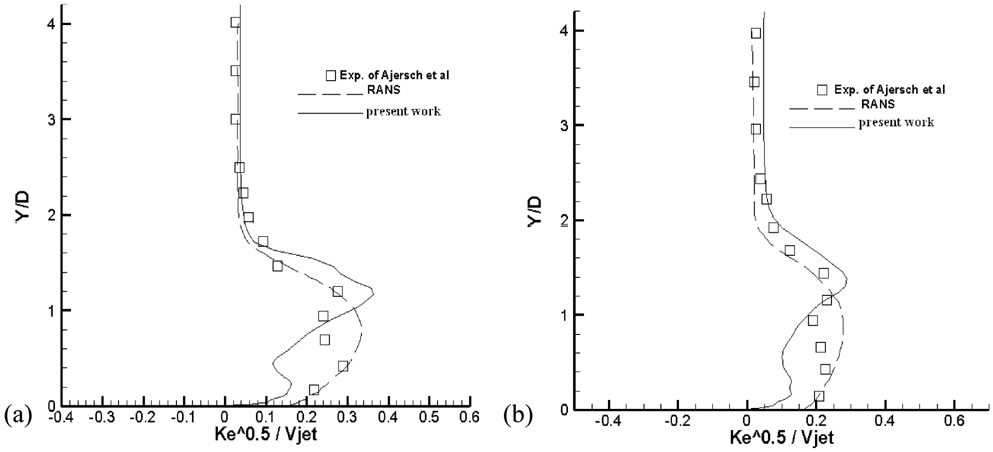

Fig. 8: Comparison of turbulence kinetic energy for different *YZ*-planes (*X/D* = (a) 5.0 and (b) 8.0) at *Z/D*= 0.0 plane

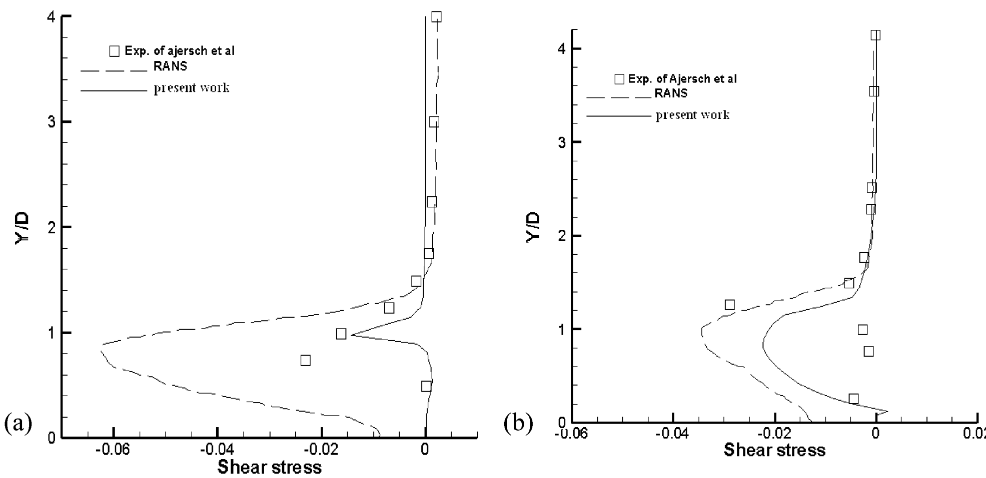

Fig. 9: Comparison of shear stress for different *YZ*-planes (*X/D*= (a) 3.0 and (b) 5.0) at *Z/D*= 0.0 plane

with Ajersch *et al*. [4] in comparison with RANS. This high accuracy may be due to the fact that the grid is stretched near the jet exit. It, therefore, reveals that the LES approach is capable to predict the swift variations near the wall while RANS has some major difficulties in this respect. Fig. 4 demonstrates the mean streamwise velocity profiles, $<\overline{V}>$, for different X locations at Z / D = -1.0. As can be seen, LES results are in good agreement with experimental ones [4] in comparison with that of by RANS and this also presents the ability of LES in predicting the fast variation near the wall. Of course, here, there are not enough existing experimental data with which to compare the authors' results. Mean streamwise velocity profiles, $<\overline{W}>$, for different X locations at Z / D = -0.5 is shown in Fig. 5; LES values are much more closer to Ajersch *et al*. [4] comparing to RANS results. Generally speaking, the present LES results are extremely close to the existing experimental ones. The flow streamlines for different *YZ*-planes (X / D = (a) 1.0, (b) 5.0) and (c) 8.0 at R = 0.5 are depicted in Fig. 6. As the distance at an X-direction from the jet exit increases, the jet flow detaches more from the wall. Therefore, as expected, at further distances from the jet exit, the Counter Rotating Vortex Pairs (CRVP) get further away from the wall. At the same time, the distance between the CRVP centres in the spanwise direction changes. Fig. 6 displays that, as the distance at an X-direction from the jet exit increases, the centres of the CRVP get further away from the wall. That is, the CRVP centres in the Y-direction are located at 0.22, 1.0 and 1.5. It is deduced that the Y-position of the CRVP centres increases when the distance from the jet exit increases. After the jet enters the cross flow, it becomes very vortical. Actually, highly strong vortical regions, i.e. the CRVP, will be formed, which will be dissipated far from the jet exit. The main influence of this vortical motion is to mix the jet with the cross flow which is really impotant in film cooling applications and pollutant dispersion, gas injection in combustors and the mixing of liquids/gases. Figs. 8 and 9 present the LES results of kinetic energy and shear stress which are in good agreement with [4] in comparison with RANS results. From the figures, it is very clear that the deviation of LES results from experimental outcomes is much lower than that of by RANS approach which approves the high ability of the present solution to simulate the turbulent jet in a cross flow.

CONCLUSION

The jet penetration and mixing characteristics of multiple square cross section jets into a cross flow on a flat plate with velocity ratio of 0.5 are studied using the LES approach. The LES results are in much better agreement with the existing experimental ones, in comparison with computational results of the RANS. After the jet enters the cross flow, it generates counter rotating vortex pairs, expands and penetrates to the cross flow in the *YZ*-plane. The results show that:

- After the jet enters the cross flow, it forms highly vortical regions, which are called Counter Rotating Vortex Pairs (CRVP).
- As the distance in an X-direction from the jet exit increases, the Y -position of the CRVP centres increases.
- The main influence of these vortical behaviours is to mix the jet with the cross flow which is used in film cooling applications and pollutant dispersion, gas injection in combustors and the mixing of liquids/gases.

As mentioned above the current numerical model has many advantages which is essentially not more complicated than the Smagorinsky model, but is constructed in such a way that its dissipation is relatively small in transitional and near-wall regions. Unlike the Smagorinsky model, the present model is able to adequately handle not only turbulent but also transitional flow. The model is expressed in first-order derivatives, does not involve explicit filtering, averaging, or clipping procedures and is rotationally invariant for isotropic filter widths.

REFERENCES

1. An eddy-viscosity subgrid-scale model for turbulent shear flow: Algebraic theory and applications, Physics of Fluids, 16: (2004) 3670-3682.
2. Andreopoulos, J., 1985. On the structure of jets in a crossflow", J. Fluid Mechanics, 157: 163-197.
3. Lee, S.W., J.S. Lee and S.T. Ro, 1994. Experimental study on the flow characteristics of streamwise inclined jets in crossflow on at plate", J. Turbomachinery, 116: 97-105.
4. Ajersch, P., J.M. Zhou, S. Ketler, M. Salcudean and I.S. Gartshore, 1995. Multiple jets in a crossflow: Detailed measurements and numerical simulations, International Gas Turbine and Aeroengine Congress and Exposition, ASME Paper 95-GT-9, Houston, Texas, USA, pp: 1-16.
5. Holdman, J.D. and R.E. Walker, 1977. Mixing of a row of jets with a confined crossflow, AIAA J., 15(2): 243-249.
6. Hoda, A. and S. Acharya, 2000. Predictions of a film coolant jet in crossflow with different turbulence models, J. Turbomachinery, 122: 558-569.
7. Keimasi, M.R. and M. Taeibi-Rahni, 2001. Numerical simulation of jets in a crossflow using different turbulence models, AIAA J., 39(12): 2268-2277.
8. Acharya, S., M. Tyagi and A. Hoda, 2001. Flow and heat transfer predictions for film cooling, Heat Transfer in Gas Turbine Systems, Annals of the New York Academy of Sci., 934: 110-125.
9. Kapadia, S., S. Roy and J. Heidmann, 2003. Detached eddy simulation of turbine blade cooling, 36th Thermophysics Conference, AIAA-2003-3632, Orlando, Florida, USA, pp: 1-10.
10. Hass, W., W. Rodi and B. Schonung, 1992. The influence of density difference between hot and coolant gas on film cooling by a row of holes: Predictions and experiments, J. Turbomachinery, 114: 747-755.
11. Honami, S., T. Shizawa and A. Uchiyama, 1994. Behaviour of the laterally injected jet in film cooling: Measurements of surface temperature and velocity/temperature filed within the jet, J. Turbomachinery, 116: 106-112.
12. Hassan, I., M. Findlay, M. Salcudean and I. Gartshore, 1998. Prediction of film cooling with compound-angle injection using different turbulence models, 6th Annual Conference of the Computational Fluid Dynamics Society of Canada, Quebec, Canada, pp: 1-6.
13. Amer, A.A., B.A. Jubran and M.A. Hamdan, 1992. Comparison of different two-equation turbulent models for prediction of film cooling from two rows of holes, Numerical Heat Transfer, Part A, 21: 143-162.
14. Thole, K., M. Gritsch, A. Schulz and S. Witting, 1998. Flow field measurements for film cooling holes with expanded exits, J. Turbomachinery, 120: 327-336.

15. Schmidt, D.L. and D.G. Bogard, 1995. Pressure gradient effects on film cooling, International Gas Turbine and Aeroengine Congress and Exposition, ASME Paper 95-GT-18, Houston, Texas, USA, pp: 1-8.
16. Ramezanizadeh, M. and M. Taeibi-Rahni, 2000. Large eddy simulation of three-dimensional cavity flow using Smagorinsky model, First International and Third Biennial Conference of the Iranian Aerospace Society, Sharif University of Technology, Tehran, Iran, 4: 99-106.
17. Ghosal, S., 1998. Mathematical and physical constraints on LES, AIAA, Paper 98-2803: 1-13.
18. Ramezanizadeh, M. and M. Taeibi-Rahni, 2002. Large eddy simulation of a two-dimensional at plate film cooling, The Ninth Asian Congress of Fluid Mechanics, Isfahan University of Technology, Isfahan, Iran, pp: 1-7.
19. Tafti, D.K., X. Zhang, W. Huang and G. Wang, 2000. Large-eddy simulations of flow and heat transfer in complex three-dimensional multilouvered fins, ASME Fluids Engineering Division Summer Meeting, FEDSM2000-11325, Boston, Massachusetts, USA, pp: 1-18.
20. Sohankar, A. and L. Davidson, 2000. Large eddy simulation of turbulent flow over a square prism by using two subgrid-scale models, 4th International and 8th Annual Conference of Iranian Society of Mechanical Engineers, Sharif University of Technology, Tehran, Iran, 3: 551-558.
21. Meneveau, C. and J. Katz, 2000. Scale-invariance and turbulence models for large-eddy simulation, Annu. Rev. Fluid Mech., 32(1).
22. Pope, S.B., 2000. Turbulent Flows (Cambridge University Press, Cambridge.
23. Smagorinsky, J., 1963. General circulation experiments with the primitive equations, Mon. Weather Rev., 91: 99.
24. Germano, M., U. Piomelli, P. Moin and W.H. Cabot, 1991. A dynamic sub-grid scale eddy-viscosity model, Phys. Fluids A 3: 1760.
25. Leonard, A., 1974. Energy cascade in large-eddy simulations of turbulent fluid flows, Adv. Geophys. 18: 237.
26. Clark, R.A., J.H. Ferziger and W.C. Reynolds, 1979. Evaluation of sub-grid scale models using an accurately simulated turbulent flow, J. Fluid Mech., 91: 1.
27. Vreman, B., B. Geurts and H. Kuerten, 1996. Large-eddy simulation of the temporal mixing layer using the Clark model," Theor. Comput. Fluid Dyn., 8: 309.
28. Vreman, B., B. Geurts and H. Kuerten, 1994. Realizability conditions for the turbulent stress tensor in large eddy simulation, J. Fluid Mech., 278: 351.